Key words: spruce wood, single-surface plasticity, characteristic length, finite element simulation

HERBERT W. MÜLLNER[*)], *CHRISTOPH KOHLHAUSER*[*)],
MARTIN FLEISCHMANN[*)], *JOSEF EBERHARDSTEINER*[*)]

INFLUENCE OF THE CHARACTERISTIC LENGTH ON THE STRENGTH PROPERTIES OF A MATERIAL MODEL FOR SPRUCE WOOD

In this contribution an overview over a numerical scheme for the crack modelling of spruce wood under tensile loading is given. A material model for biaxially stressed spruce wood with consideration of the effect of knots on the strength properties has been developed. A necessary feature of this material model is its ability to treat cracks by means of the so-called smeared crack concept. For this reason the consideration of a so-called characteristic length in the corresponding evolution laws of the strength values is required. The successful implementation in the material model is shown by means of various numerical examples.

1. Introduction

In wood the development of cracks due to tensile loading can be observed. Cracking is described as local damage causing a loss of continuity between material points of an area where the tensile strength of the material is exceeded. The finite element method is based on the algebraic form of a weak formulation of the underlying boundary value problem. In the case of cracking, the displacement fields exhibits discontinuities in the analytical solution. To preserve the continuity of the displacement field in the finite element solution, a discrete crack is homogenised and simulated by plastic strains distributed over a finite width.

*) *Institute for Mechanics of Materials and Structures, Vienna University of Technology, Vienna, Austria; E-mail:* Herbert.Muellner@tuwien.ac.at; ej@imws.tuwien.ac.at

In the presented material model the so-called smeared crack concept is used. This fictitious crack concept uses the entire element domain for the representation of a discrete crack. The crack behaviour is considered in terms of stress-strain relationships. The advantage of this concept is that the knowledge of the directions of the cracks is not required. According to this, the used finite element mesh of the investigated structure needs not to be modified.

This paper is structured as follows: In Chapter 2 a motivation for the consideration of different post failure behaviour is given. In Chapter 3 the main idea of the so-called characteristic length is summarised. Chapter 4 refers to the consideration of the characteristic length in the present material model. The identification of critical values of the characteristic length due to the material is given in Chapter 5. In Chapter 6 a numerical example shows the influence of different sizes of finite elements on the post failure behaviour of a simple beam. Chapter 7 shows the results of numerical investigations of two wooden structures. The paper will be completed by conclusions.

2. Motivation

In this section it will be shown why a material model for wood should consider different post failure behaviour due to cracks depending on the discretisation of the structure. As example a simple beam with two concentrated loads (see Figure 1) is considered.

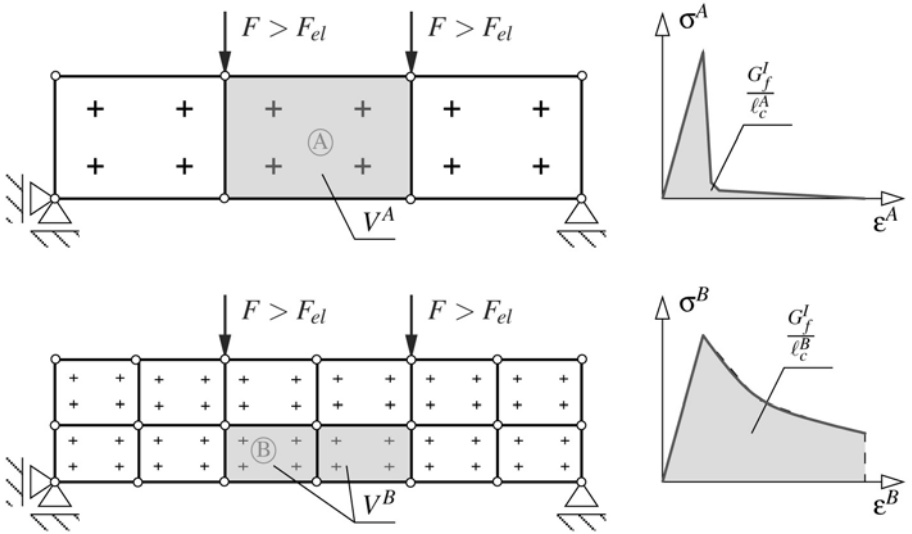

Figure 1 - Different finite element meshes for the simulation of a simple beam with two concentrated loads

In this situation pure bending in the middle of the beam will occur. Thus, no shear failure will develop. If the loads are larger than the elastic limit of this beam, a tension crack on the bottom side in the middle of the beam will occur.

If a numerical simulation of this situation is done by means of a course finite element mesh (case *A*) then the crack will occur in the middle element which has a certain volume V^A. In the respective stress-strain diagram the crack will lead to strength softening. Thus, because of the crack development a certain value of energy is saved in the material which depends on the constant energy release rate G_f^I.

When using a finer mesh (case *B*) for the simulation, the whole volume of the elements, where the crack occurs, is smaller than in case *A*. Thus, the decrease of the strength in the stress-strain diagram must not be as large as in case *A*. Assuming the energy release rate G_f^I is a material parameter, information concerning the size of the involved finite elements is needed. Therefore a so-called characteristic length of the respective element is introduced which fulfils the energy balance equation for both finite element meshes as:

$$E = V^A \frac{G_f^I}{\ell_c^A} = V^B \frac{G_f^I}{\ell_c^B} \Rightarrow V^A \ell_c^B = V^B \ell_c^A \qquad (1)$$

3. Crack modelling by means of the characteristic length

The situation described in Chapter 2 reveals one disadvantage of softening cracking models and the resulting influence of the size of finite elements on the numerical results.

In this context OLIVER [8] proposed to introduce a characteristic length and to consider the crack band width using a stress-strain relationship. Following this concept the displacements are continuous and the corresponding gradients are discontinuous along a singular line in a two-dimensional domain which can be defined as material line (see Figure 2 (a)).

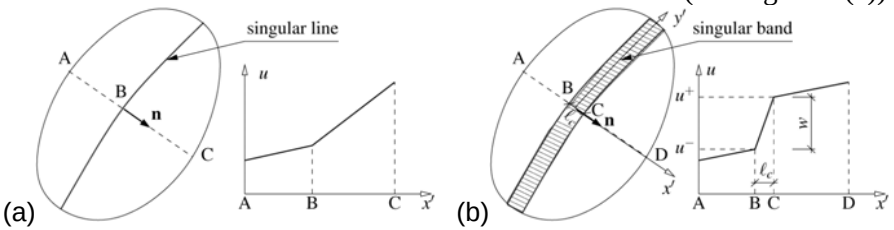

Figure 2 - Crack as (a) singular line in a continuous medium and (b) singular band between two singular lines adapted from [8]

A singular line representing a discontinuity in the displacement field can only be modelled by means of the edge of a standard finite element with C^0 continuity, because on nodes displacements results are available. However, a crack produces discontinuities in displacements and in displacement gradients. Thus, a crack can be modelled as the distance of two singular lines (see Figure 2 (b)). The area limited by these two singular lines is called singular band. The width of the singular band represents the characteristic length ℓ_c.

OLIVER [8] contemplated displacement and traction vectors as well as energy dissipation in the singular band and identified an equation for the determination of the characteristic length ℓ_c in a finite element mesh using the standard shape functions for an element. For further details see OLIVER [8].

4. Consideration in the material model for spruce wood

In MÜLLNER et al. [7] the concept and the properties of a single-surface plasticity model for the simulation of spruce wood under multiaxial loading are summarised. The extension of this material model for consideration of specific wood properties such as knots was done by MÜLLNER et al. [6].

The formulation of a non-associated hardening and softening rule allows the consideration of several modes of failure identified with the results of the experimental investigation performed by EBERHARDSTEINER [1]. The used yield surface is shown in Figure 3.

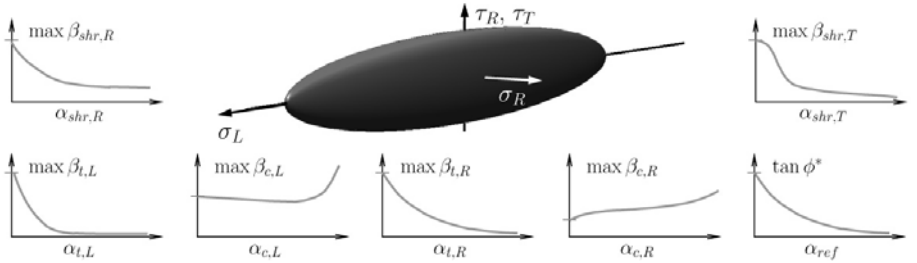

Figure 3 - Yield surface of single-surface material model in the orthotropic stress space and evolution laws for the strength values depending on the strain-like primary variables α_i

The formulation of the seven evolution laws, also shown in Figure 3, requires seven control variables. These so-called primary variables are collected in a vector $\boldsymbol{\alpha}$. The determination of $\boldsymbol{\alpha}$ is subjected to non-associated hardening and softening rules. Because of the brittle tensile and the ductile compression behaviour of wood the formulation of such rules is required. The seven evolution laws affect different modes of failure:

- brittle tensile failure in fibre direction,
- compressive failure with densification in fibre direction,
- brittle tensile failure perpendicular to grain,
- ductile compressive behaviour with densification perpendicular to grain,
- reduction of a strength ratio which relates the tilt of the yield surface,
- failure due to in-plane shear in a plane perpendicular to the *LR*-plane, and
- failure due to transverse shear.

Within this material model the characteristic length ℓ_c is considered in the dimensionless material parameter $k_{i,j}$ ($i \in \{t,c\}$, $j \in \{L,R\}$) in every evolution law which affects softening by means of a crack.

4.1 Evolution laws of strength values

The evolution laws of the four main strength values, the tensile and compressive strength in and perpendicular to fibre direction of the aforementioned material model for the orthotropic material wood will be discussed in this section.

For brittle tensile failure in longitudinal direction the decrease of the strength value $\beta_{t,L}$ due to plastic loading is considered as

$$\max \beta_{t,L} = \max {\beta_{t,L}}^{0} e^{-k_{t,L}\alpha_{t,L}} \quad \text{with} \quad k_{t,L} = \frac{\max {\beta_{t,L}}^{0}\, \ell_c}{{G_{f,L}}^{I}}\,, \qquad (2)$$

where ${G_{f,L}}^{I}$ is the mode I fracture toughness of wood for the longitudinal direction and $\alpha_{t,L}$ is a strain-like primary variable (see Section 4.2) which affects plastic tensile loading in fibre direction. Due to numerical problems the maxima of all strength values are used for the formulation of the evolution laws. These maxima do not coincide with the uniaxial strength values.

For compressive failure in longitudinal direction the decrease of the strength value $\beta_{c,L}$ due to plastic loading is considered to be

$$\max \beta_{c,L} = \max {\beta_{c,L}}^{0} - Y_{1,L}\left(1 - e^{-k_{c,L}\alpha_{c,L}}\right) - q_L(\alpha_{c,L}) \quad \text{with} \quad k_{t,L} = \frac{\max {\beta_{t,L}}^{0}\, \ell_c}{{G_{fc,L}}^{I}}\,, \qquad (3)$$

where ${G_{fc,L}}^{I}$ is the fracture energy density and $\alpha_{c,L}$ is the primary variable which affects plastic compressive loading in fibre direction. $Y_{1,L}$ is the part of the strength value which is influenced by plastic loading. q_L denotes the densification stress. For compressive loading in fibre direction the development of an initial crack has been observed by the experiments performed by EBERHARDSTEINER [1]. Thus, a small dependence on the characteristic length is considered in the model for this strength function.

For brittle tensile failure in radial direction the decrease of the strength value $\beta_{t,R}$ due to plastic loading is considered to be

$$\max \beta_{t,R} = \max {\beta_{t,R}}^{0} e^{-k_{t,R}\alpha_{t,R}} \quad \text{with} \quad k_{t,R} = \frac{\max {\beta_{t,R}}^{0}\, \ell_c}{{G_{f,R}}^{I}}\,, \qquad (4)$$

where ${G_{f,R}}^{I}$ is the mode I fracture toughness for the radial direction and $\alpha_{t,R}$ is the primary variable which affects plastic tensile loading perpendicular to fibre direction.

The last strength value in the *LR*-plane affects the compressive failure in radial direction. In this case hardening occurs. Thus, the increase of the strength value $\beta_{c,R}$ due to plastic loading is considered to be

$$\max \beta_{c,R} = \max {\beta_{c,R}}^{0} + Y_{1,R}\left(1 - e^{-k_{c,R}\alpha_{c,R}}\right) - q_R(\alpha_{c,R}) \quad \text{with} \quad k_{c,R} = \text{const.}\,, \qquad (5)$$

where $\alpha_{c,R}$ is the primary variable which affects plastic compressive loading perpendicular to fibre direction. Again, $Y_{1,R}$ is the part of the strength value which is influenced by plastic loading and q_R denotes the densification stress. In the case of compressive loading in radial direction no dependence on the characteristic length is implemented in the model, because no crack development has been observed.

More theoretical descriptions of the different parameters can be found in MACKENZIE-HELNWEIN et al. [4, 5].

The characteristic length ℓ_c has a significant influence on the macroscopic behaviour of the material model. The post-failure behaviour as described by equations (2) to (5) is shown in Figure 4 for different values of ℓ_c. The right plots show the discussed strength functions $\beta_{i,j}$ over the strain-like primary variable $\alpha_{i,j}$ ($i \in \{t,c\}$, $j \in \{L,R\}$). The left images show the initial and modified yield surfaces when plastic loading is reached for the corresponding strength function.

In the case of tensile loading both the corresponding strength values in and perpendicular to fibre direction decrease. The bigger the size of the elements the stronger the decrease of the affected strength value will occur. Because of the development of straight cracks parallel to grain, a decrease of nearly the total strength will occur. This leads to numerical problems when accomplishing numerical simulations of timber structures with components of dominant tensile loading [3]. Thus, a finer finite element mesh is necessary for such simulations.

Tension in longitudinal direction:

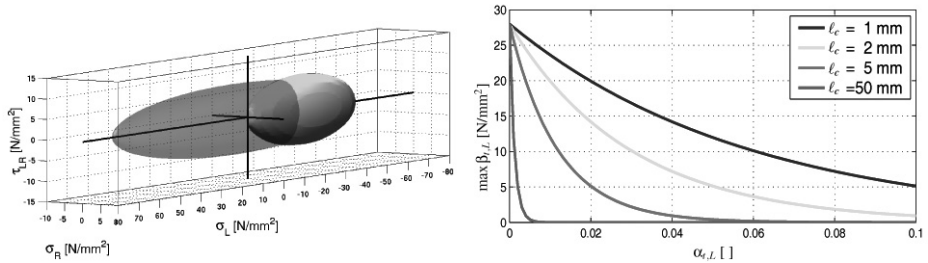

Compression in longitudinal direction:

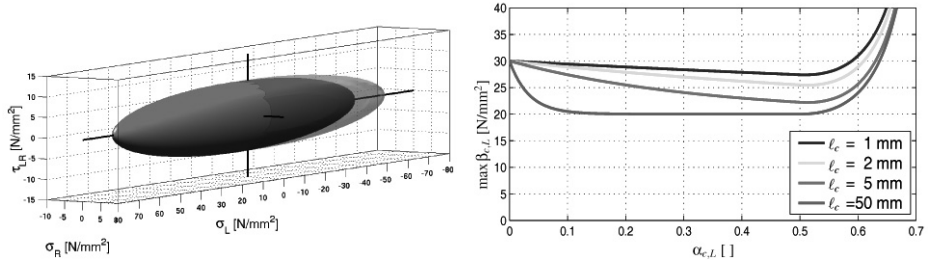

Tension in radial direction:

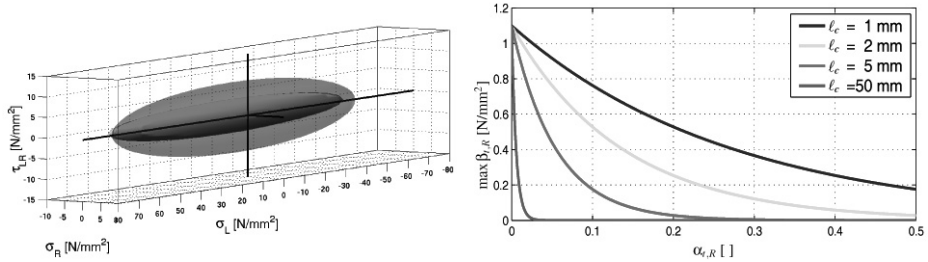

Compression in radial direction:

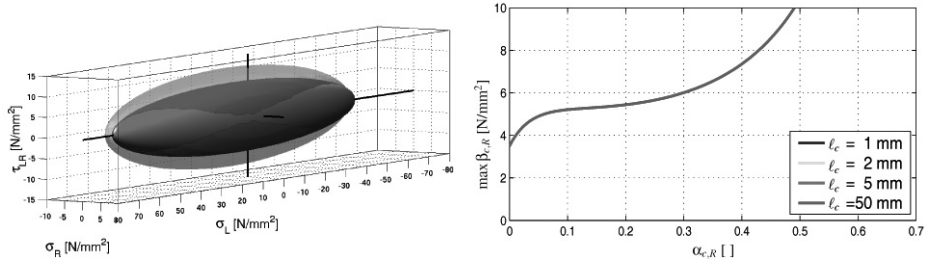

Figure 4 - Initial and modified yield surfaces and plots of different strength functions over corresponding primary variable α_i with dependence on various characteristic lengths ℓ_c

4.2 Interpretation of the strain-like primary variables

All softening functions in equations (2), (3) and (4) use the following form to describe the post-failure behaviour of spruce wood for the observed failure modes:

$$\beta_{i,j}\left(\alpha_{i,j}\right) = \beta^0 \, e^{-k_{i,j}\,\alpha_{i,j}} \quad . \tag{6}$$

These functions are based on an exponential decrease of the initial strength value $\beta_{i,j}^{\,0}$, the factors $k_{i,j}$ and $\alpha_{i,j}$ ($i \in \{t,c\}$, $j \in \{L,R\}$) given for each evolution law. The strain-like parameter $\alpha_{i,j}$ is defined as

$$\alpha = \frac{w}{\ell_c} \quad , \tag{7}$$

where w is the crack opening.

One can plot the loss of strength either with respect to the crack opening w or the strain-like parameter $\alpha_{i,j}$ [3]. Figure 5 shows the softening behaviour for these two representations. In this figure the softening function for the tensile strength in longitudinal direction is evaluated, even though the validity of these graphs is general. The softening functions of other strength values, however, differ in material parameters, which influence the position and curvature of the exponential function. For a given strength value, the softening function is only governed by ℓ_c.

As pointed out in Chapter 3, when modelling a crack, one has to find a way to deal with the numerical problems emanating from the discontinuity in the displacement field due to a crack. The characteristic length ℓ_c is the extension of a domain over which a crack opening w will be distributed as an equivalent plastic strain in a smeared crack model. ℓ_c may be the length of a finite element perpendicular to the crack direction.

The interpretation of α is therefore depending on the chosen representative dimension of the finite element mesh. It can be interpreted as an equivalent crack strain. For a given crack opening w the corresponding value of α depends on the characteristic length and therefore on the dimension of the used finite element mesh.

This can be seen in Figure 5, where the area under the function in the lower graph is identical regardless of the characteristic length and thus always equal to the fracture toughness G_f^I, because the crack opening w does not include any information on the discretisation.

In the upper graph of Figure 5 the softening function is plotted against the strain-like variable α. This figure identifies the different post-failure behaviour due to different characteristic lengths ℓ_c, i.e. the chosen finite element discretisation.

The area under the function is equal to the fracture toughness divided by the characteristic length and is therefore smaller for higher values of ℓ_c.

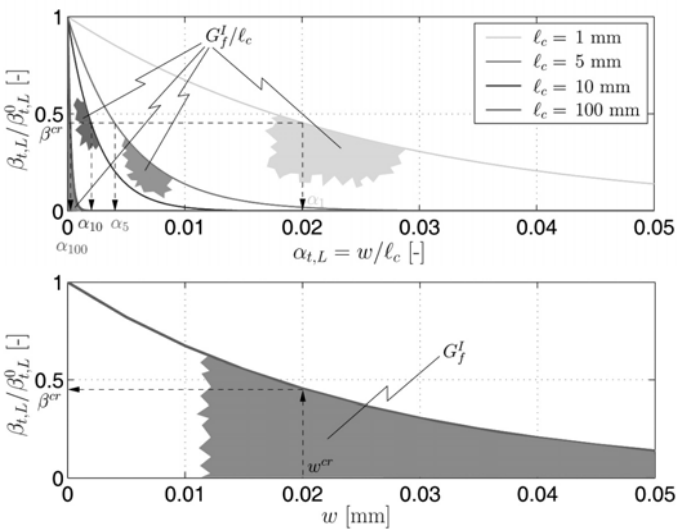

Figure 5 - Strength softening with respect to crack opening width w and strain-like primary variable α for tensile loading in grain direction

A larger factor $k_{i,j}$ leads to a stronger and therefore faster degradation of strength as the crack opens. Therefore, a higher value for the ratio β^0 / G_f^I and a larger characteristic length ℓ_c, e.g. a coarser finite element mesh, have the same influence on the softening behaviour.

5. Uniaxial critical characteristic length

Uniaxial investigations of MACKENZIE-HELNWEIN et al. [4] showed that there is an upper limit for the characteristic length. If the resulting ℓ_c is larger than this limit, hardening will occur despite the development of a crack. Consideration of a physically relevant behaviour of the model yields to the following equations for the critical characteristic length:

$$\ell_{c,crit,L} = \frac{E_L \, G_{f,L}{}^I}{\left(\beta_{t,L}{}^0\right)^2} \quad \text{and} \quad \ell_{c,crit,R} = \frac{E_R \, G_{f,R}{}^I}{\left(\beta_{t,R}{}^0\right)^2} \,, \tag{8}$$

where E_L and E_R are the young's moduli in and perpendicular to grain. Analysing (8) for typical values of spruce wood [5] yields to $\ell_{c,crit,L}$ = 4.7 mm and $\ell_{c,crit,R}$ = 10.1 mm. In KOHLHAUSER [3] the derivation of equation (8) is included. Figure 6 shows the elasto-plastic stiffness

$$\mathbb{C}_{ep,j} = \frac{E_j \, H_j}{E_j + H_j} \quad \text{with} \quad H_j = -\left(\beta_{t,j}{}^0\right)^2 \frac{\ell_{c,j}}{G_{f,j}{}^I} \quad \text{for} \quad j \in \{L, R\} \tag{9}$$

after crack initiation over the characteristic length for tensile loading in longitudinal and radial direction. This value must be negative for softening. In order to fulfil this condition a finer finite element mesh has to be chosen. For multiaxial loading of a structure the critical characteristic length lies between the two given limits for the longitudinal and radial direction.

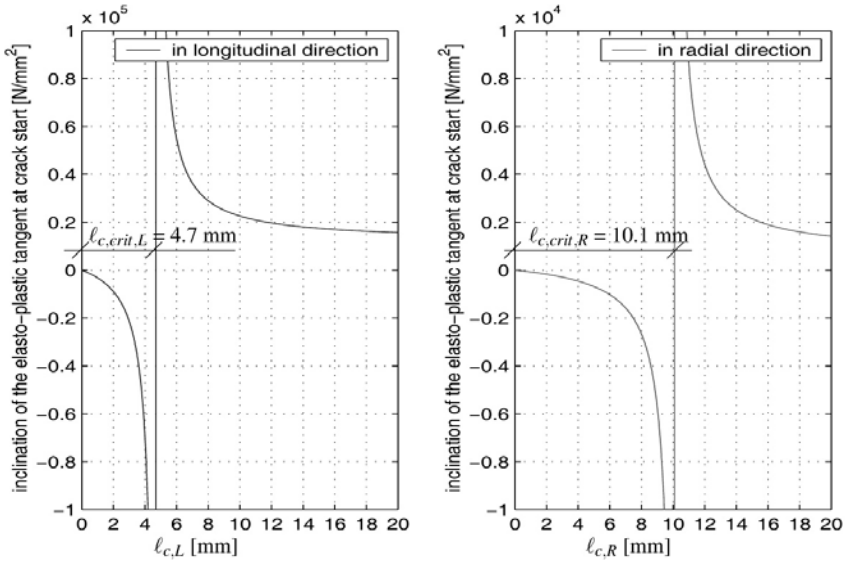

Figure 6 - Dependence of the inclination of the elasto-plastic tangent at the start of the crack development on the characteristic length

The strong influence of the characteristic length on the numerical model behaviour and the critical characteristic length can be clearly laid out in a stress-strain diagram as shown in KOHLHAUSER [3]. Figure 7 shows the post-failure behaviour of the tensile strength in fibre direction with respect to α and the corresponding stress-strain curves for different values of the characteristic length.

The linear-elastic regime is independent of the finite element mesh. After the stress reaches the maximum strength, the strength decreases at an exponential rate according to the softening function.

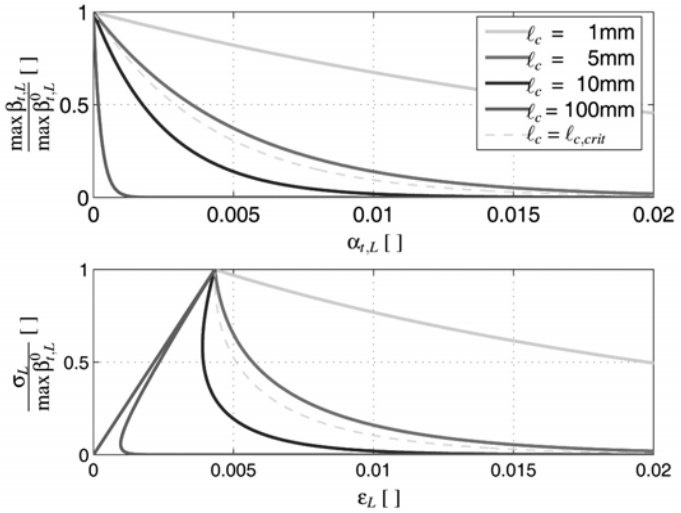

Figure 7 - Softening behaviour and stress-strain curve for tensile strength in fibre direction for the critical and other characteristic lengths

For sufficiently small values of ℓ_c there is only one unique solution. For higher values of ℓ_c the solution may become non-unique. This regime of non-unique solutions causes numerical instability of the material model and must not be reached in any computation. The last stress-strain curve that exhibits a unique solution defines the value of the critical characteristic length.

The values of the critical characteristic length of the evolution laws of the four main strength values of the material model follow from equation (8). Depending on the material parameters E_i, $G_{f,i}$ and β_i higher values occur for compression direction and very small values appear in tensile direction. The values are given in Table 1.

The finite element sizes in a given discretisation must not exceed these critical values to ensure a stable material model behaviour. The infinity of the critical characteristic length of the evolution law for compressive strength perpendicular to the fibre direction corresponds with the statements of Section 4.1.

Table 1: Values of the critical characteristic length according to [3]

corresponding evolution law	$\ell_{c,crit}$ [mm]
longitudinal tensile strength	5.9
longitudinal compressive strength	1503.0
radial tensile strength	12.3
radial compressive strength	∞

6. Numerical example

The influence of the characteristic length on the results of numerical simulations will be shown in a small example. As shown in Fig. 8, a beam divided into two zones is considered. Therefore, a beam is divided into two zones. The properties of the first part are modelled by the mentioned material model, the second part is considered to behave linear elastic. Thus, failure has to occur in the first part. By increasing the prescribed horizontal displacements $\bar{u}$ a tension crack will appear in the first part. The variation of the dimension a leads to different values for the characteristic lengths ℓ_c and to different paths of the stress-strain-relationship in the post failure domain.

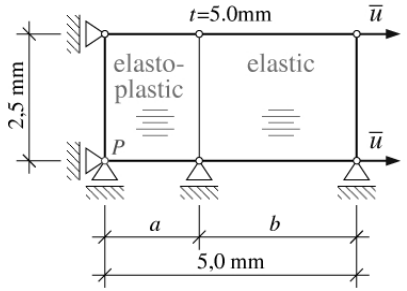

Figure 8 - Dimensions of a beam strained by horizontal displacements

The results for the point P of this numerical simulation are depicted in form of stress-strain diagrams for the in Figure 9. It shows the different decrease of strength which is subject to the dimension of the left element. The biggest dimension a leads to the fastest decrease of strength.

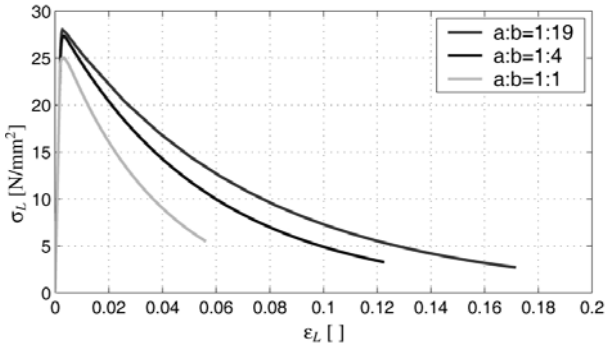

Figure 9 - Stress-strain diagram for point P of the numerical example

The faster the strength decreases after reaching the elastic limit of the structure the bigger the numerical problems. To avoid such problems finer load increments and smaller dimensions of the finite elements are required. The smaller the dimensions of the finite elements are the more realistic is the prognosis of the responding stresses in the structure. Minor differences of the maximum fibre stress are a consequence of different finite element meshes. However, the presented concept only refers to the material behaviour and considers the influence of different element size on the strength properties of the material. The softening behaviour of tensile loading in longitudinal direction is detected accurately.

7. Experimental validation of the material model

In order to verify the performance of the developed material model it is necessary to compare experimental and numerical results. As a first example a small bone-shaped specimen has been tested and numerically analysed [6]. In addition, an experimental validation of the constitutive model by means of structured size test was performed [2].

7.1 Example 1 – gluelam beam with a circular opening

To predict the ultimate load of structures characterised by a brittle failure mechanism, gluelam beams with three different sizes of circular openings were chosen. Each configuration consists of three beams, loaded with a single force (deformation controlled) in the middle of the beam. The openings are situated approximately in the quarter points of the span width of the beams. They have diameters of d = 0.2 h, 0.3 h, 0.4 h, respectively (dimensions of the beam: length x height (h) x width: 4.00 x 0.45 x 0.12 m). Fig. 4 (a) shows one configuration of the nine experiments. In Fig. 4 (b) the load-displacement diagram for series 04 (d = 0.4 h) is given. The ultimate load, predicted with a finite element simulation using the proposed material model fits well to the data obtained by the experiments.

7.1 Example 2 – wooden break joint

For the second test series a structure with a ductile failure mechanism was chosen to investigate the plastic behaviour of spruce wood for dominating loading situations perpendicular to grain. A simple truss consisting of three truss members was manufactured three times. The joints were done by step joints. All tests were performed by a displacement controlled vertical movement of the tie. Fig. 5 (a) shows one configuration of the experiments and in Fig. 5 (b) the corresponding load-displacement diagram for the tie is drawn.


(a)

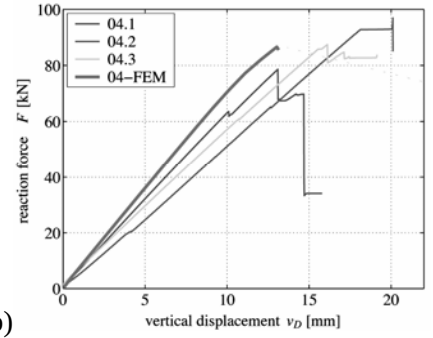

(b)

Figure 10 - Gluelam beam with a circular opening
(a) configuration of the experiment, (b) load-displacement diagram


(a)

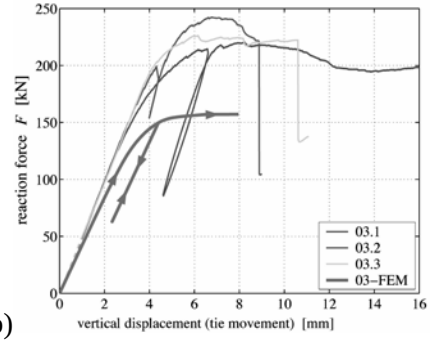

(b)

Figure 11 - Wooden break joint
(a) configuration of the experiment, (b) load-displacement diagram

With the proposed elasto-plastic material model realistic simulations of structures of biaxially stressed spruce wood can be carried out. The verification of the material model was performed successfully by means of comparison of Finite Element simulations and corresponding structural tests. The obtained differences between numerical prediction and experimental results for example 1 are in a common statistical spread in timber engineering. For example 2 the obtained poor agreement can be explained due to the appearance of big strains for compressive loading in radial direction, which cannot be considered because of the restriction of small strains in the material model. More details of these numerical simulations can be found in FLEISCHMANN [2].

8. Conclusions

Wood as an orthotropic material is characterised by a brittle behaviour due to tensile loading in and perpendicular to grain. Therefore, after reaching the elastic limit of the structure, a tension crack will appear locally. To simulate such parts of timber structures the consideration of a crack concept in the material model is necessary. In this context the so-called smeared crack concept is used. It influences the corresponding stress-strain diagrams and needs no knowledge of the directions of the cracks. Therefore no mesh modifications are required. With a numerical simulation of a simple beam the functionality of the implemented smeared crack concept was shown.

The influence of the characteristic length in the softening behaviour has been identified. Discretisation of structures needs to be performed with element sizes smaller than the critical characteristic length, which are in the range of a few millimetres for tension loading, to ensure a stable material model behaviour.

9. References

[1] Eberhardsteiner J.: Mechanisches Verhalten von Fichtenholz – Experimentelle Bestimmung der biaxialen Festigkeitseigenschaften, 2002, Springer, Vienna, in German.

[2] Fleischmann M.: Numerische Berechnung von Holzkonstruktionen unter Verwendung eines realitätsnahen orthotropen elasto-plastischen Werkstoffmodells, 2005, PhD Thesis, Vienna University of Technology, in German.

[3] Kohlhauser Ch.: A Multi-Surface Plasticity Model with Strain Softening for Failure Mechanisms of Clear Spruce Wood under Plain Biaxial Stress Conditions and Stabilization of its Numerical Implementation for Large Characteristic Lengths, 2005, Master's Thesis, Vienna University of Technology.

[4] Mackenzie-Helnwein P., Eberhardsteiner J., Mang H.A.: A Multi-Surface Plasticity Model for Clear Wood and its Application to the Finite Element Analysis of Structural Details. Computational Mechanics, 2003, Vol. 31, pp. 204-218.

[5] Mackenzie-Helnwein P., Müllner H.W., Eberhardsteiner J., Mang, H.A.: Analysis of Layered Wooden Shells using an Orthotropic elasto-plastic Model for multi-axial Loading of Clear Spruce Wood. Computer Methods of Applied Mechanics and Engineering, 2005, Vol. 194, pp. 2661-2685.

[6] Müllner H.W., Fleischmann M., Eberhardsteiner J.: Orthotropic Single-Surface Plasticity Model for Spruce Wood including the Effect of Knots. The Archive of Mechanical Engineering, 2005, Vol. 52, pp. 253-265.

[7] Müllner H.W., Mackenzie-Helnwein P., Eberhardsteiner J.: Constitutive Modelling of Clear Spruce Wood under Biaxial Loading by Means of an Orthotropic Single-Surface Model under Consideration of Hardening and Softening Mechanisms. Proceedings of the 2nd International Symposium on Wood Machining, 2004, pp. 83 - 90.

[8] Oliver J.: A Consistent Characteristic Length for Smeared Cracking Models. International Journal for Numerical Methods in Engineering, 1989, Vol. 28, pp. 461-474.

10. List of symbols

V	[mm^3]	volume of a finite element
E	[J]	energy of a finite element
w	[mm]	crack opening
ℓ_c	[mm]	characteristic length of a finite element
$\ell_{c,crit}$	[mm]	critical characteristic length
$G_{f,L}^{I}$	[N/mm]	mode I fracture toughness for longitudinal direction
$G_{fc,L}^{I}$	[N/mm]	fracture energy density
$G_{f,R}^{I}$	[N/mm]	mode I fracture toughness for radial direction
i	[ ]	index identifying tensile or compressive loading
j	[ ]	index identifying longitudinal of radial direction
$\beta_{i,j}$	[N/mm^2]	material strength function
$k_{i,j}$	[ ]	material parameter for evolution law
$\alpha_{i,j}$	[ ]	strain-like primary variable
$Y_{1,j}$	[N/mm^2]	strength value influenced by plastic loading
q_j	[N/mm^2]	densification stress
E_L	[N/mm^2]	young's modulus in longitudinal direction
E_R	[N/mm^2]	young's modulus in radial direction